

Entanglement generation in never interacting spins via reservoir engineering

Josephine Dias,^{1,*} Christopher W. Wächtler,² Kae Nemoto,^{1,3} and William J. Munro^{4,3}

¹*Quantum Information Science and Technology Unit,*

Okinawa Institute of Science and Technology Graduate University, Onna-son, Okinawa 904-0495, Japan

²*Department of Physics, University of California, Berkeley, California 94720, USA*

³*National Institute of Informatics, 2-1-2 Hitotsubashi, Chiyoda, Tokyo 101-0003, Japan.*

⁴*NTT Basic Research Laboratories & NTT Research Center for Theoretical Quantum Physics, NTT Corporation, 3-1 Morinosato-Wakamiya, Atsugi, Kanagawa 243-0198, Japan.*

(Dated: June 14, 2023)

The generation and preservation of entanglement is a central goal in quantum technology. Traditionally, dissipation in quantum systems is thought to be detrimental to entanglement, however dissipation can also be utilised as a means of generating entanglement between quantum spins that are not directly interacting. In particular entanglement can be generated between two qubits, or multi qubit systems via a collective coupling to a reservoir. In this work, we explore multiple spin domains pairwise coupled to different reservoirs and show that entanglement can be generated between spins which are not coupled to each other, or even coupled to the same reservoir.

I. INTRODUCTION

Quantum entanglement enables quantum computation and communication that surpass their classical counterparts in various tasks [1–6]. Therefore, the generation and preservation of entanglement represents a significant goal within the field of quantum technology. Typically, dissipative effects are known to be detrimental to quantum entanglement [7], and significant efforts are made into isolating the quantum system from its environment. However, the environment can also be used as a means of generating entanglement between different quantum systems [8–12].

With recent advancements in hybrid quantum systems, we can engineer both the system *and* the environment to perform the task we are interested in [13–16]. Such hybrid systems can involve many different elements, from solid state to atomic, molecular and optical [17–19]. Hybrid quantum systems naturally provide a rich environment to study complex phenomena in open quantum systems [20]. Our focus in this work is the behaviour of many spin ensembles collectively coupled to bosonic reservoirs and the entanglement that can be generated through this system. The collective coupling of multiple spins to the same bath has been shown as a mechanism to transfer excitations between spins [21–23] and also as a means to charge quantum batteries [24]. Furthermore multiple spin domains pairwise coupled to multiple reservoirs can transfer excitations to and from domains which are not directly coupled [25].

Open quantum systems form a complex and dynamic backdrop to study the generation and dynamics of entanglement (see Ref. [26] for a review). It is known that entanglement can be generated between two qubits via the interaction of the qubits with the same reservoir [9–11, 27–32] or the interaction of two oscillators with the

same reservoir [33]. A collective coupling to a common bath can also be used to generate entanglement between multiple spins [12] and spin domains [22], even if the reservoir is in a thermal state [10, 11]. For instance, a system of two spin domains collectively coupled to the same bosonic reservoir was explored and its steady state was shown to have entanglement between spin-domains [22].

In order to illustrate the mechanism by which initially separable systems can become entangled via a collective coupling to a reservoir, consider an elementary example of two spins A and B collectively coupled to the same bath and initialised in the separable state $|\psi\rangle_{AB} = |\uparrow\rangle_A \otimes |\downarrow\rangle_B$. This state can also be written as $|\psi\rangle_{AB} = \frac{1}{\sqrt{2}}(|\Psi^+\rangle_{AB} + |\Psi^-\rangle_{AB})$ which is an equal superposition of the symmetric triplet state $|\Psi^+\rangle_{AB}$ and antisymmetric singlet state $|\Psi^-\rangle_{AB}$. With a zero-temperature reservoir coupling, the triplet state decays to the ground state $|\downarrow\rangle_A \otimes |\downarrow\rangle_B$, however the singlet state cannot decay. Therefore, the steady state for this system is [9]

$$\rho_{AB} = \frac{1}{2}(|\downarrow\rangle_A |\downarrow\rangle_B \langle\downarrow|_A \langle\downarrow|_B + |\Psi^-\rangle_{AB} \langle\Psi^-|_{AB}) \quad (1)$$

and this is an entangled state between spins A and B . If we were to quantify the amount of entanglement in this state, we could use the entanglement of formation [34–36] (see Sec. III) which for this two-qubit state is $E_F \approx 0.354$, that is 0.354 ebits. We emphasise here that the spins were not initially entangled, nor did they evolve according to a Hamiltonian coupling individual spins. The entanglement present in the steady state of (1) is solely due to the relaxation of the spins via their collective reservoir coupling.

To go beyond this simple example of two spins, consider the system depicted in Fig. 1 (a) (which is the system considered in Refs. [21, 22]). Here we have a system of N_A spins in domain A , and a single spin in domain B . With this system initialised in the state of

$$|\psi\rangle_{AB} = |\uparrow\uparrow \cdots \uparrow\rangle_A \otimes |\downarrow\rangle_B \quad (2)$$

* josephine.dias@oist.jp

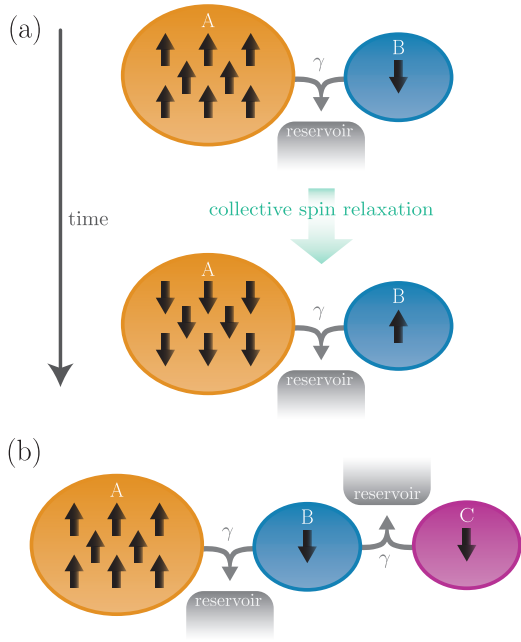


Figure 1. Collective spin relaxation via a collective coupling to a bosonic reservoir can be used to transfer excitations between spins. (a) The double domain system of Ref. [21, 22] (b) Three spin domains pairwise coupled to two reservoirs.

after collective spin relaxation (for a zero-temperature bath), the steady state will be

$$|\psi\rangle_{AB} = |\downarrow\downarrow\cdots\downarrow\rangle_A \otimes |\uparrow\rangle_B \quad (3)$$

in the limit of $N_A \rightarrow \infty$. That is, through the collective coupling of the spins to the bosonic reservoir, the steady state of domain B is excited even though it initially started in its ground state [21, 22]. As can be seen from (3), the steady state in the limit of $N_A \rightarrow \infty$ is separable. However, for finite N_A , collective spin relaxation produces entanglement in the steady state between domains A and B . In fact, the logarithmic negativity [37, 38] for the steady state peaks for a spin population of $N_A = 5$ and has a value of $E_N \approx 0.55$ [22].

To illustrate how we can extend the model of Fig. 1(a) in Ref. [21, 22], consider the system depicted in Fig. 1(b): In addition to the two spin domains of Fig. 1(a) we add another spin domain C collectively coupled with domain B to a second reservoir. That is, domains A and B are collectively coupled to the same reservoir and domains B and C are collectively coupled to a different reservoir. For an initial state of

$$|\psi\rangle_{ABC} = |\uparrow\uparrow\cdots\uparrow\rangle_A \otimes |\downarrow\rangle_B \otimes |\downarrow\rangle_C \quad (4)$$

we can expect that for N_A sufficiently large, the coupling to the first reservoir will result in the spins in A relaxing to the ground state and the single spin in B will move to its excited state. For large N_A , domains A and B will relax at a time that scales with $1/N_A$ due to the superradiant decay [39, 40]. We can then consider the

coupling to the second reservoir. In this case, the single spin in B will be excited (for large N_A) and the single spin in C has already been initialised in its ground state. With the collective coupling to the second reservoir, we can expect these two spins to end in an entangled state. In fact, for $N_A \rightarrow \infty$, we can expect the relaxation of B and C to proceed to the steady state described in equation (1) which is an entangled state with entanglement of formation $E_F = 0.354$, that is 0.354 ebits.

In this work we explore the generation of entanglement through multiple spin domains with multiple reservoir couplings. Unlike previous works investigating entangling qubits through interaction with a common reservoir [9–11, 27–32], we will show here generation of entanglement between two spins in separate domains which have never interacted and are not even coupled to the same reservoir. In particular, we will also see the amount of entanglement (between qubits not coupled to the same reservoir) to be of similar level to that of the previously mentioned example of two qubits collectively coupled to the same zero temperature reservoir. This paper is arranged in the following way: In Sec. II we present details of the model considered in this work. In Sec. III, we use that model to analyse the capabilities of our system to distribute entanglement. We then look at how entanglement distribution is affected by realistic conditions such as individual decay, dephasing and thermal reservoirs in Sec. IV. Finally, we will also show how multiple system-reservoir couplings can be used to generate tripartite entangled states in Sec. V, before presenting our summary and conclusions in Sec. VI.

II. OUR MODEL

The system we examine in this work consists of M separate spin domains, each consisting of N_m identical spin-1/2 particles with frequency $\omega_0/2\pi$. Although in our system, we assume each spin has the same energy, entanglement can still be generated through a common environment when this is not the case [41]. The spins in two neighbouring spin domains are collectively coupled to a bosonic reservoir. Additionally, our system is symmetric under exchange of two spin-1/2 particles in a given spin domain. The Hamiltonian for our system of M spin domains and $M - 1$ reservoirs is given by:

$$H = \hbar\omega_0 \sum_m J_m^z + \sum_m \sum_{k_i}^{M-1} \hbar\omega_{k_i} a_{k_i}^\dagger a_{k_i} + \sum_m \sum_{k_i}^{M-1} \left[t_{k_m} (J_m^+ + J_{m+1}^+) a_{k_m} + t_{k_m}^* a_{k_m}^\dagger (J_m^- + J_{m+1}^-) \right] \quad (5)$$

where the operators $a_{k_m}^\dagger$ (a_{k_m}) are the creation (annihilation) operators of the k_m^{th} bosonic mode of the reservoirs with frequency $\omega_{k_m}/2\pi$. The operators J_i^α are the collective spin operators for the m^{th} spin domain and are

given by $J_m^\alpha = 1/2 \sum_{n_m=1}^{N_m} \sigma_{n_m}^\alpha$ where $\sigma_{n_m}^\alpha$ are the n_m^{th} Pauli spin operators with $\alpha = x, y, z$. The collective spin raising and lowering operators for the m^{th} spin domain are $J_m^\pm = J_m^x \pm iJ_m^y$. In (5), the first term represents the Hamiltonian of the spin domains, the second term represents the Hamiltonian of the bosonic reservoirs and the third term represents the interaction between the spin domains and the reservoirs. In the third term, each term in the sum over $M - 1$ reservoirs describes the coupling between the m^{th} and $(m + 1)^{\text{th}}$ spin domain which are collectively coupled to the m^{th} bosonic reservoir, with t_{k_m} ($t_{k_m}^*$) representing the emission (absorption) amplitudes that fix the spectral density of the reservoirs, $\Gamma_m(\omega) = 2\pi \sum_{k_m} |t_{k_m}|^2 \delta(\omega - \omega_{k_m})$. Within the Born-Markov-secular approximation, the master equation in the rotating frame can be written as [20, 42–44]:

$$\dot{\rho}_s = \sum_i^{M-1} \frac{\gamma_i}{2} \mathcal{D} [J_m^- + J_{m+1}^-] \rho_s, \quad (6)$$

for bosonic reservoirs at zero temperature with $\mathcal{D}[O]\rho = 2O\rho O^\dagger - O^\dagger O\rho - \rho O^\dagger O$. Previous work has experimentally implemented a double spin domain system coupled to a common resonator where each spin domain consisted of nitrogen-vacancy (NV) ensembles in diamonds [45]. In this work, we primarily consider the case of three spin domains coupled to two reservoirs and therefore our master equation is given specifically by:

$$\dot{\rho}_s = \frac{\gamma}{2} \mathcal{D} [J_A^- + J_B^-] \rho_s + \frac{\gamma}{2} \mathcal{D} [J_B^- + J_C^-] \rho_s \quad (7)$$

where we have used the same reservoir coupling constant γ for all system-reservoir couplings. Further, we can introduce a scaled time $\gamma t/2$ to simplify our considerations.

III. ENTANGLEMENT DYNAMICS

In this work, we extend the results of Ref. [22] to more than two spin domains with more than one reservoir coupling. We will show here that entanglement can be generated not just through collective coupling to the same reservoir but also through a chain setup where entanglement will be generated between spins which are not coupled to the same reservoir.

To begin, we will consider here the situation where domains A and C consist of a single spin in each domain, while the central domain B has N_B spins. This is depicted in Fig. 2. Our goal is to entangle the qubits (in domains A and C) which are not coupled to the same reservoir. After this system evolves in time according to equation (7), through collective spin relaxation, entanglement is generated between all the spins, however, here we primarily focus on the entanglement between the two single spins in domains A and C. In the remainder of this paper, we will examine how to maximise the entanglement between spins in A and C as well as how robust this entanglement is to realistic imperfections.

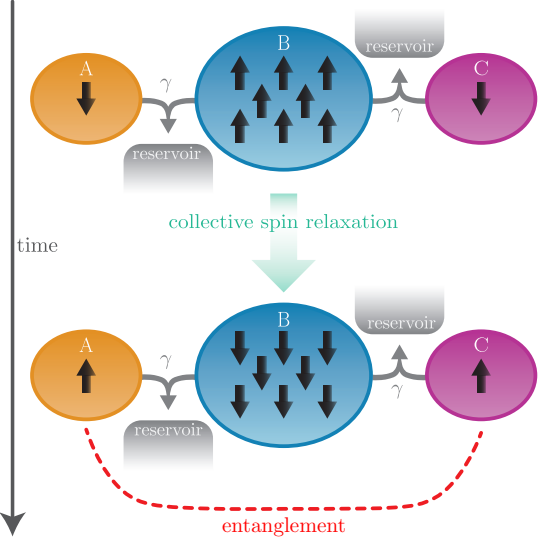


Figure 2. Three spin domains pairwise coupled to two separate reservoirs at zero temperature. Collective relaxation of the spins produces entanglement between the spins. Entanglement between spins in outer domains is maximised for a configuration with a large number of spins in the middle domain.

Our initial state configuration is:

$$|\psi_{\text{in}}\rangle = |\downarrow\rangle_A \otimes |\uparrow \cdots \uparrow\rangle_B \otimes |\downarrow\rangle_C \quad (8)$$

which is depicted in the top part of Fig. 2. However, different initial state configurations can still produce entanglement (see Appendix). After our initial state (8), evolves in time we then trace out the spins in domain B leaving us with the reduced density matrix $\rho_{AC} = \text{Tr}_B[\rho]$ of the state of the two spins, one in domain A and one in domain C. To measure the amount of entanglement present in the state ρ_{AC} , we will use the entanglement of formation, which quantifies the minimum amount of pure state entanglement needed to prepare the state [34]. For an arbitrary state of two qubits, this quantity is given by [36]:

$$E_F(\rho) = \mathcal{E}(C(\rho)) \quad (9)$$

where \mathcal{E} is given by $\mathcal{E}(C) = h([1 + \sqrt{1 - C^2}]/2)$ with $h(x) = -x \log_2 x - (1 - x) \log_2 (1 - x)$. The concurrence C is given by $C(\rho) = \max\{0, \lambda_1 - \lambda_2 - \lambda_3 - \lambda_4\}$ where λ_i are the square roots of the eigenvalues of the matrix $\rho \tilde{\rho}$ with $\tilde{\rho} = (\sigma_y \otimes \sigma_y) \rho^* (\sigma_y \otimes \sigma_y)$ [35].

In Fig. 3(a) we plot the entanglement generation dynamics between the two spins in domains A and C as well as the relaxation dynamics of the initially excited domain B. Here we can see that as the number of spins in domain B increases, the decay time decreases. This is indicative of the collective effect of superradiance [39, 40] where the radiation is enhanced and sped up in the presence of multiple emitters. The increase in spin domain size also contributes to enhanced entanglement dynamics

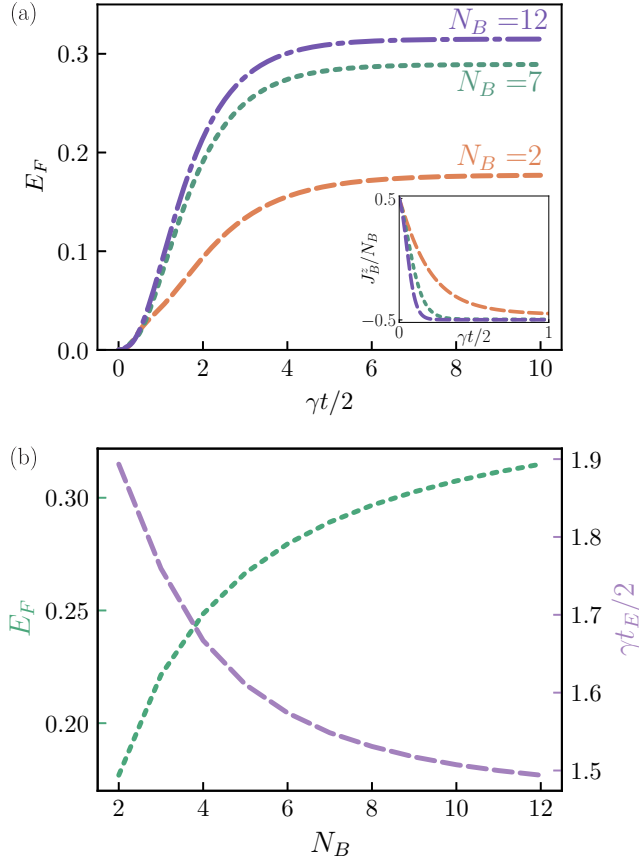


Figure 3. Entanglement generated between spins in A and C using the configuration shown in Fig. 2. (a) The entanglement of formation E_F versus the scaled time $\gamma t/2$ for various values of N_B (the spin-population in domain B) which clearly shows the entanglement generation is higher and faster for large N_B . Further, shown in the inset is the normalised collective spin relaxation J_B^z/N_B illustrating the enhanced decay dynamics due to superradiance [39, 40]. (b) Steady state entanglement E_F and speed of entanglement generation $\gamma t_E/2$ as a function of the spin-population N_B . The left axis shows the steady state entanglement of formation E_F generated between spins in A and C (green, dotted line). The right axis shows the value of $\gamma t_E/2$ where t_E is the time it takes for entanglement between A and C to reach half of its maximum value (purple, dashed line).

- that is the speed of entanglement generation is increased as is the amount of entanglement present between qubits in A and C . Note that only collective dissipation into a zero temperature reservoir is governing the dynamics, and for this case, the entanglement present in the steady state remains and does not decay. We also emphasise here that entanglement is generated between spins which are not coupled to the same reservoir. For the system size of $N_B = 12$, the entanglement generated between spins in domains A and C is $E_F \approx 0.315$ ebits. This is noteworthy because it is a comparable amount of entanglement to that which is generated via collective decay with spins coupled to the *same* zero-temperature reservoir.

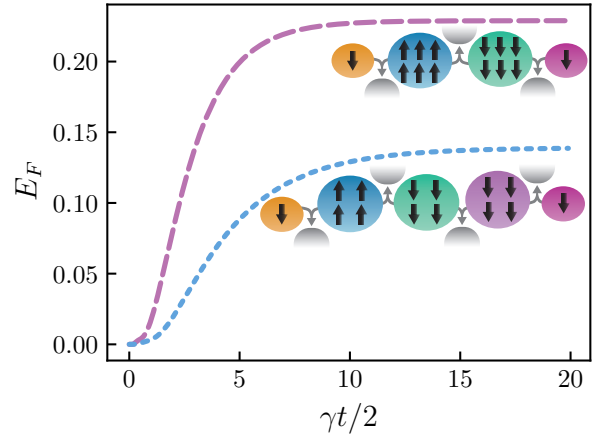


Figure 4. The entanglement of formation E_F generated between spins in the outer domain of a spin domain chain versus the scaled time $\gamma t/2$. The pink (dashed) line shows E_F for spins in the outer domains of a four spin domain chain connected with three reservoirs, depicted in the inset shown in the upper right corner. The spin domain population configuration for this result is $\{N_A, N_B, N_C, N_D\} = \{1, 6, 6, 1\}$. The blue (dotted) line shows the E_F for spins in the outer domains of a five spin domain chain with four reservoirs, depicted in the inset diagram below the blue (dashed) line. The spin domain population configuration for this result is $\{N_A, N_B, N_C, N_D, N_E\} = \{1, 4, 4, 4, 1\}$.

Next in Fig. 3(b), we plot the maximum value of the entanglement of formation E_F (reached at steady state) as well as the value of $\gamma t_E/2$ where t_E is the time for entanglement between A and C to reach half of the maximum entanglement present during the system evolution. It can clearly be seen that the entanglement distribution is enhanced (more entanglement and faster distribution) for a large spin domain size in B . Results here are limited to small total system sizes ($N_A + N_B + N_C$) due to the memory required to simulate the combined system. As can be seen from Fig 3(b) as we increase N_B , the increase in entanglement is rapid at first, however the growth steadily slows. Thus, for even bigger N_B the payoff with increased entanglement between A and C will not be significant.

While the previous results focus on distributing entanglement between spins in the outer domains of a three spin domain chain, entanglement generation through collective spin relaxation is not limited to three domains. In Fig. 4 we present results for the entanglement between the single spins in the outer domains of spin domain chains consisting of four (pink, dashed line) and five (blue, dotted line) spin domains. These dynamics use the initial state depicted in the inset diagrams in Fig. 4 respectively, that is all spins initialised in the ground state with the exception of domain B which has all spins initialised in the excited state. While we only show entanglement for a single spin domain population configuration for four and five domains, as before, entanglement

between outer qubits is maximised for larger spin populations of the middle domains. Here, we have constrained the total number of spins in all middle domains to be the same (12 spins), however the top line uses 12 spins split between two spin-domains and the bottom line uses 12 spins split between three spin-domains. These results are limited due to the total size of the system however, they show that entanglement can be distributed between qubits separated by two or three spin domains which are in turn connected by collective coupling to three or four reservoirs. For this result, as is the case with the previous results, the only effect taken into account in this model is collective decay into zero-temperature reservoirs. In this case, we observe constant entanglement which does not decay in the steady state.

IV. INDIVIDUAL DECAY AND DEPHASING

The results contained in previous section are interesting but represent the highly specific and idealized sys-

tem of collective relaxation with a zero-temperature bath and with no other individual effects present. It is important to consider more realistic models, which includes effects such as dephasing, individual spin relaxation and non-zero temperature reservoirs, and examine how these aspects may alter the previously observed entanglement generation.

For the three domain system depicted in Fig. 2, we now incorporate finite temperature reservoirs as well as dephasing and individual relaxation. This yields the following master equation, again in the rotating frame of the system [46]:

$$\begin{aligned} \dot{\rho}_s = & \frac{\gamma}{2} (\bar{n} + 1) (\mathcal{D} [J_A^- + J_B^-] \rho_s + \mathcal{D} [J_B^- + J_C^-] \rho_s) + \frac{\gamma}{2} \bar{n} (\mathcal{D} [J_A^+ + J_B^+] \rho_s + \mathcal{D} [J_B^+ + J_C^+] \rho_s) \\ & + \sum_{i_{A,B,C}=1}^{N_{A,B,C}} \frac{\gamma}{2} (\bar{n} + 1) \mathcal{D} [\sigma_{i_{A,B,C}}^-] \rho_s + \frac{\gamma}{2} \bar{n} \mathcal{D} [\sigma_{i_{A,B,C}}^+] \rho_s + \frac{\gamma_{\text{dep}}}{2} \mathcal{D} [\sigma_{i_{A,B,C}}^z] \rho_s \end{aligned} \quad (10)$$

In (10), the first and second terms correspond to the collective thermalisation between the pairs of spin domains (A and B , B and C respectively) and the thermal reservoir. Associated with that reservoir is the Bose-Einstein distribution $\bar{n} = 1 / (e^{\hbar\omega_0/k_B T} - 1)$ for a given temperature T and with Boltzman constant k_B . Next, the third and fourth terms in (10) correspond to individual thermalisation of the spins. Finally, the last term corresponds to dephasing. To summarise, the first line in (10) corresponds to collective effects while the second line corresponds to individual effects associated with thermalization and dephasing. Note that the individual and collective thermalisation occurs with the same system-reservoir coupling constant γ .

In Fig. 5(a), we plot the entanglement dynamics of the original system with no dephasing (pink, dashed line) as well as the entanglement between spins in domains A and C with various dephasing rates of $\gamma_{\text{dep}}/\gamma$ (broken lines). We observe a reduction in peak entanglement generated through the system-bath evolution in time but also a gradual reduction in the entanglement present in the steady state. For the results in Fig. 5(a), the dephasing is the only additional effect present, the reservoirs remain at zero temperature ($\bar{n} = 0$) and there is no individual decay.

We then examine the entanglement generation capa-

bilities of our system under the effects of individual spin coupling to the reservoir. In this case, the spins all have individual as well as the collective dissipation. Again, we shall keep the bosonic reservoir to zero temperature to isolate the effect of individual decay on entanglement dynamics. We find that individual coupling has a significant detrimental effect on the entanglement present. Shown in Fig. 5(b) is the entanglement dynamics between single spins in domains A and C . Note the significantly smaller scale of the y-axis in Fig. 5(b) relative to the other results in this work. The maximum entanglement of formation produced in this case is $E_F = 0.0039$. Note that as the system size increases (number of spins), the superradiant collective effects occur on a much faster time scale than the individual one and most likely dephasing. For example in NV centers in diamond, the collective relaxation can be of order of microseconds, while the individual one is 10 orders of magnitude larger [47].

Lastly, the temperature of the thermal reservoir also substantially affects the entanglement generated through this system. Shown in Fig. 5(c) is the entanglement dynamics between qubits in A and C for thermal reservoirs of various temperatures for spin domain population of $N_B = 11$. For this result, we keep only collective spin-reservoir coupling to the bath. As can be seen in Fig. 5(c), the entanglement generated through our sys-

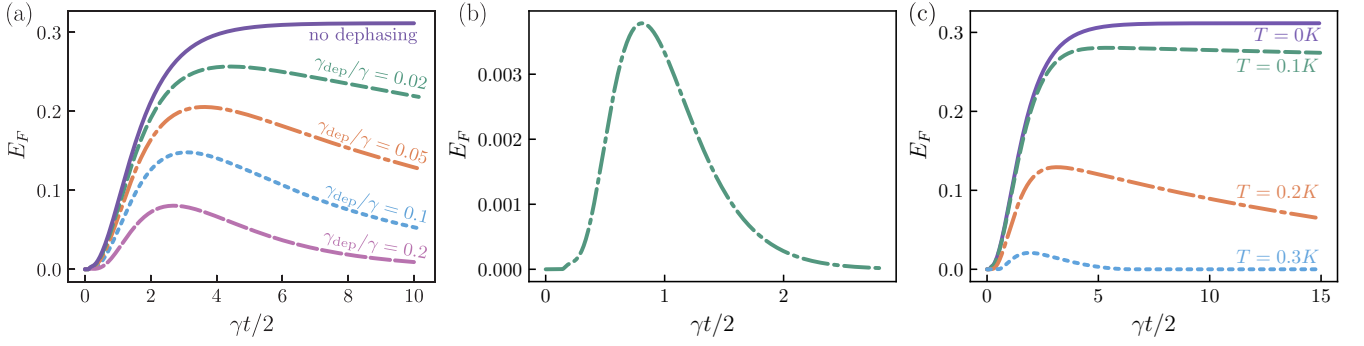


Figure 5. The entanglement of formation E_F generated between spins in domains A and C versus the scaled time $\gamma t/2$ with a spin population of $N_B = 11$ in domain B . In (a), we show various dephasing rates γ_{dep} . The pink (long dashed) line shows the effect of dephasing with $\gamma_{\text{dep}}/\gamma = 0.2$, the blue (dotted) line uses $\gamma_{\text{dep}}/\gamma = 0.1$, the orange (dash-dot) line uses $\gamma_{\text{dep}}/\gamma = 0.05$, the green (dashed) line uses $\gamma_{\text{dep}}/\gamma = 0.02$, and the purple (solid) line shows the ideal case of $\gamma_{\text{dep}}/\gamma = 0$. In (b), we show the entanglement dynamics with both collective and individual decay. In (c), we use a thermal reservoir of temperature T with the following parameters chosen: $\omega_0/2\pi = 10$ GHz and $\gamma = 0.01$ Hz.

tem is highly sensitive to the temperature of the thermal reservoirs. As the temperature increases, less entanglement is generated and in the steady state entanglement is also reduced.

We have seen in this section the impact of realistic effects on entanglement distribution via collective dissipation with multiple spin domains and reservoirs. While it is clear that entanglement can still be generated between spins in domains A and C , it significantly decreases if individual decay or finite temperatures are taken into account. Further, the constant, non-decaying entanglement in the steady state observed in Sec. III is no longer present once any of these effects are taken into account. In the results of Figs. 5(a)-(c) we observe a decline in the entanglement of formation over time. However, individual process are always detrimental to entanglement between spins, and therefore the decay of the entanglement in the results of Fig. 5 is to be expected.

V. TRIPARTITE NEGATIVITY

The previous results in this work focused solely on entangling two qubits through collective spin relaxation with multiple collective spin-reservoir couplings. In this section, we will show how this same process can be utilised to generate tripartite entanglement between three spins. Consider the setup shown in Fig. 6(a). This set up is reminiscent of a spin-star configuration [48, 49] but we emphasise again the spins are not directly coupled, merely collectively coupled to the same reservoir as other spins. Here, a central spin-domain (labelled D) contains many spins and is collectively coupled to three bosonic reservoirs with three other spin-domains each containing a single spin only (labelled A , B and C). The system is initialised in the separable state:

$$|\Psi\rangle = |\downarrow\rangle_A \otimes |\downarrow\rangle_B \otimes |\downarrow\rangle_C \otimes |\uparrow\uparrow \cdots \uparrow\rangle_D \quad (11)$$

Under the process of collective dissipation with the reservoir setup illustrated by the diagram in Fig. 6(a), the steady state of A , B and C (with domain D traced out) is given by:

$$\rho_{ABC} = \text{Tr}_D [\rho_{ABCD}] = c_G |\downarrow\downarrow\downarrow\rangle \langle \downarrow\downarrow\downarrow| + c_W |W\rangle \langle W| \quad (12)$$

that is, the steady state of the reduced system of three qubits A , B and C is a mixture of the ground state and the W -state which is $|W\rangle = 1/\sqrt{3} (|\uparrow\downarrow\downarrow\rangle + |\downarrow\uparrow\downarrow\rangle + |\downarrow\downarrow\uparrow\rangle)$. Therefore, the steady state of this reduced system has tripartite entanglement between the three remaining qubits. In order to demonstrate the presence of tripartite entanglement in the steady state of this system, we calculate the tripartite negativity, defined as the geometric mean of the negativities of all bipartitions [50]:

$$\mathcal{N}_{ABC}(\rho) = (\mathcal{N}_{A|BC} \mathcal{N}_{B|AC} \mathcal{N}_{C|AB})^{1/3} \quad (13)$$

where each of the terms $\mathcal{N}_{i|jk}$ are the bipartite negativities between subsystems i and jk given by $\mathcal{N}(\rho) = (|\rho^{\Gamma_i}| - 1)/2$ with ρ^{Γ_i} corresponding to the partial transpose of the density matrix with respect to subsystem i and $\|X\|$ is the trace norm of the operator X given by $\|X\| = \text{Tr} \sqrt{XX^\dagger}$ [37, 51]. Note that with this definition of the bipartite negativity, maximally entangled Bell states have the negativity of 0.5. Further, for three qubit entangled states, GHZ states yield a tripartite negativity of 0.5 but W states have a tripartite negativity of 0.47. In Fig. 6(b), we give the tripartite negativity generated via the configuration shown in Fig. 6(a) with reservoirs at zero-temperature and no individual effects. The dynamics show clear presence of tripartite negativity in the steady state. For the given spin-domain population of $N_D = 11$, the steady state tripartite negativity is $\mathcal{N}_{ABC} \approx 0.043$. Additionally, the inset shows the steady state tripartite entanglement for various values of N_D , the population of the central domain. As the spin-domain population of D grows, the steady state contribution of

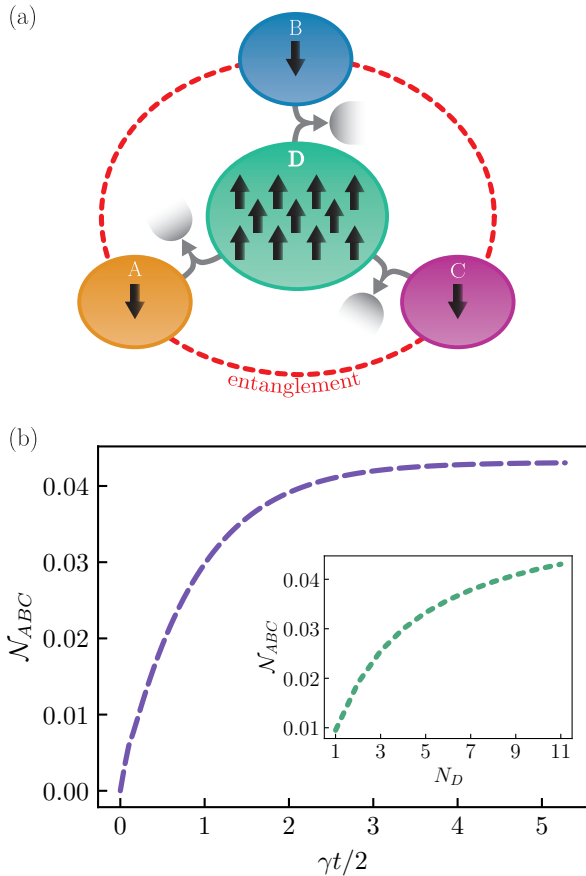


Figure 6. Tripartite quantum correlations generated from collective decay with multiple reservoirs. (a) Initially, all spins are in a separable state (11) with their configuration depicted here. After collective spin relaxation, the reduced state of the three single qubits in spin-domains A, B and C are entangled in the steady state. (b) Tripartite negativity generated between spins A, B and C during spin relaxation with the configuration pictured in (a) for a central domain populated with $N_D = 11$ spins. Shown in the inset is the steady state tripartite negativity for spin population N_D ranging from 1 to 11.

the W-state term [c_W in (12)] grows larger, and thus the tripartite negativity is maximised for large N_D . However, while this increase is rapid at first, it slows as N_D continues to increase indicating less payoff in tripartite correlations for further increasing the size of the central domain D . Nevertheless, the results here show the generation of tripartite correlations between three qubits not coupled to each other or even the same reservoir.

VI. SUMMARY AND CONCLUSIONS

We have shown here how, by utilising reservoir engineering, and with a completely separable initial state, entanglement can be generated between two spins which are not coupled to each other or even coupled to the same

reservoir. We have focused mostly here on the case where the two spins collectively decay into different reservoirs with a single common spin domain collectively decaying into both reservoirs. For this case, the entanglement is maximised for a large number of spins in the central domain. The speed of entanglement generation is also maximised for a larger spin population in the central domain. Additionally, the entanglement between the qubits not coupled to the same reservoir, can approach the level of entanglement generated when two qubits are collectively coupled to the same zero-temperature reservoir. Entanglement generation via this mechanism is not limited to the three spin-domain case, but can also occur between qubits in the outer domains of four and five domain systems as well as entangling three qubits using a large central domain of many spins.

The results in Sec. IV show that, as expected, when realistic effects are taken into account the entanglement generation between spins suffers significantly. With dephasing or individual spin-reservoir coupling, not only is the maximum entanglement generated reduced, the entanglement in the steady state also decays over time. However, we emphasise that for large enough ensemble size, the collective effects will occur on a timescale that is much faster than that of the individual effects. Additionally, finite temperature reservoirs also reduce the maximum entanglement and cause the steady state entanglement to decay. While the results here predict rather small entanglement generation, further optimisation may significantly increase the maximum entanglement of qubits and make it more robust against imperfections.

VII. ACKNOWLEDGEMENTS

C. W. W. acknowledges financial support by the Deutsche Forschungsgemeinschaft (DFG, German Research Foundation) – Project No. 496502542 (WA 5170/1-1). This work was supported by the JSPS KAKENHI Grants 19H00662 & 21H04880, the MEXT Quantum Leap Flagship Program (MEXT QLEAP) Grant JPMXS0118069605 and the Moonshot R&D Program Grant JPMJMS226C.

APPENDIX

In Sec. III we showed the dynamics of entanglement generation in our three spin-domain system with the initial state $|\psi_{\text{in}}\rangle = |\downarrow\rangle_A \otimes |\uparrow \cdots \uparrow\rangle_B \otimes |\downarrow\rangle_C$ where the middle and most populated spin domain B is initialised with all spins in the excited state. However, this is not the only configuration that can produce entanglement through collective spin relaxation. In Fig. 7 we give the entanglement dynamics for the following initial state

$$|\psi_{\text{in}}\rangle = |\uparrow\rangle_A \otimes |\downarrow \cdots \downarrow\rangle_B \otimes |\downarrow\rangle_C. \quad (\text{A.14})$$

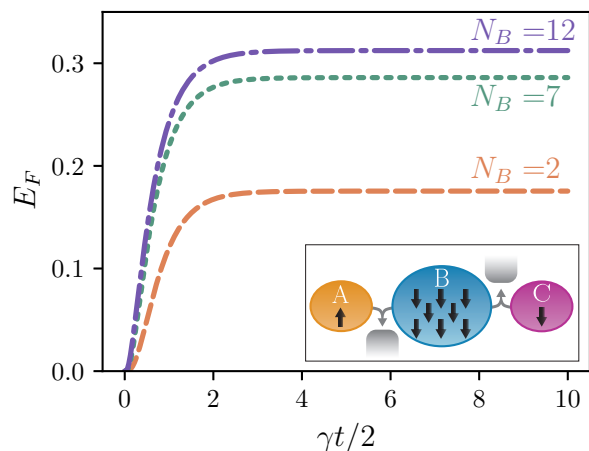


Figure 7. Entanglement of formation generated via collective spin relaxation using the initial state where the single spin in domain A is in its excited state while the spins in domains B and C are in their ground state. This state given in (A.14) is depicted in the inset. The generated entanglement of formation E_F versus scaled time $\gamma t/2$ is given for $N_B = 2, 7, 12$. We clearly observe the maximal E_F increases as N_B increases.

Again, this is the entanglement of formation between the single spins in domains A and C after the spins in B have been traced out. Here, only one spin is initialised in the excited state and that is the single spin in domain A . The maximum entanglement generated from initial state A.14 is slightly lower than that generated from initial state (8). However, the system reaches half of the maximum steady state entanglement slightly faster for initial condition A.14 than (8).

-
- [1] G. Vidal, Efficient Classical Simulation of Slightly Entangled Quantum Computations, *Physical Review Letters* **91**, 147902 (2003).
 - [2] A. Ekert and R. Jozsa, Quantum algorithms: entanglement-enhanced information processing, *Philosophical Transactions of the Royal Society of London. Series A: Mathematical, Physical and Engineering Sciences* **356**, 1769 (1998).
 - [3] D. Gottesman and I. L. Chuang, Demonstrating the viability of universal quantum computation using teleportation and single-qubit operations, *Nature* **402**, 390 (1999).
 - [4] R. Raussendorf and H. J. Briegel, A One-Way Quantum Computer, *Physical Review Letters* **86**, 5188 (2001).
 - [5] N. Gisin and R. Thew, Quantum communication, *Nature Photonics* **1**, 165 (2007).
 - [6] R. Jozsa and N. Linden, On the role of entanglement in quantum-computational speed-up, *Proceedings of the Royal Society of London. Series A: Mathematical, Physical and Engineering Sciences* **459**, 2011 (2003).
 - [7] K. Życzkowski, P. Horodecki, M. Horodecki, and R. Horodecki, Dynamics of quantum entanglement, *Physical Review A* **65**, 012101 (2001).
 - [8] A. K. Rajagopal and R. W. Rendell, Decoherence, correlation, and entanglement in a pair of coupled quantum dissipative oscillators, *Physical Review A* **63**, 022116 (2001).
 - [9] M. Hor-Meyll, A. Auyuanet, C. V. S. Borges, A. Aragão, J. A. O. Huguenin, A. Z. Khoury, and L. Davidovich, Environment-induced entanglement with a single photon, *Phys Rev A* **80**, 042327 (2009).
 - [10] D. Braun, Creation of Entanglement by Interaction with a Common Heat Bath, *Physical Review Letters* **89**, 277901 (2002).
 - [11] M. S. Kim, J. Lee, D. Ahn, and P. L. Knight, Entanglement induced by a single-mode heat environment, *Physical Review A* **65**, 040101 (2002).
 - [12] S. Schneider and G. J. Milburn, Entanglement in the steady state of a collective-angular-momentum (Dicke) model, *Physical Review A* **65**, 042107 (2002).
 - [13] F. Verstraete, M. M. Wolf, and J. Ignacio Cirac, Quantum computation and quantum-state engineering driven by dissipation, *Nature Physics* **5**, 633 (2009).
 - [14] M. Keck, D. Rossini, and R. Fazio, Persistent currents by reservoir engineering, *Phys. Rev. A* **98**, 053812 (2018).
 - [15] F. m. c. Damanet, E. Mascarenhas, D. Pekker, and A. J. Daley, Controlling quantum transport via dissipation engineering, *Phys. Rev. Lett.* **123**, 180402 (2019).
 - [16] Y. Yanay and A. A. Clerk, Reservoir engineering of bosonic lattices using chiral symmetry and localized dissipation, *Physical Review A* **98**, 043615 (2018).
 - [17] G. Kurizki, P. Bertet, Y. Kubo, K. Mølmer, D. Petrosyan, P. Rabl, and J. Schmiedmayer, Quantum technologies with hybrid systems, *Proceedings of the National Academy of Sciences* **112**, 3866 (2015).
 - [18] M. Wallquist, K. Hammerer, P. Rabl, M. Lukin, and P. Zoller, Hybrid quantum devices and quantum engineering, *Physica Scripta* **2009**, 014001 (2009).
 - [19] Z.-L. Xiang, S. Ashhab, J. Q. You, and F. Nori, Hybrid quantum circuits: Superconducting circuits interacting with other quantum systems, *Reviews of Modern Physics* **85**, 623 (2013).
 - [20] H. P. Breuer and F. Petruccione, *The Theory of Open Quantum Systems* (Oxford University Press, Oxford, 2002).
 - [21] Y. Hama, W. J. Munro, and K. Nemoto, Relaxation to Negative Temperatures in Double Domain Systems, *Physical Review Letters* **120**, 060403 (2018).
 - [22] Y. Hama, E. Yukawa, W. J. Munro, and K. Nemoto, Negative-temperature-state relaxation and reservoir-assisted quantum entanglement in double-spin-domain

- systems, *Physical Review A* **98**, 052133 (2018).
- [23] P. Stegmann, J. König, and B. Sothmann, Relaxation dynamics in double-spin systems, *Physical Review B* **101**, 075411 (2020).
 - [24] J. Q. Quach and W. J. Munro, Using Dark States to Charge and Stabilize Open Quantum Batteries, *Phys. Rev. Appl.* **14**, 024092 (2020).
 - [25] J. Dias, C. W. Wächtler, V. M. Bastidas, K. Nemoto, and W. J. Munro, Reservoir-assisted energy migration through multiple spin domains, *Physical Review B* **104**, L140303 (2021).
 - [26] L. Aolita, F. d. Melo, and L. Davidovich, Open-system dynamics of entanglement: a key issues review, *Reports on Progress in Physics* **78**, 042001 (2015).
 - [27] S. Oh and J. Kim, Entanglement between qubits induced by a common environment with a gap, *Physical Review A* **73**, 062306 (2006).
 - [28] L. D. Contreras-Pulido and R. Aguado, Entanglement between charge qubits induced by a common dissipative environment, *Physical Review B* **77**, 155420 (2008).
 - [29] S. Maniscalco, F. Francica, R. L. Zaffino, N. Lo Gullo, and F. Plastina, Protecting Entanglement via the Quantum Zeno Effect, *Physical Review Letters* **100**, 090503 (2008).
 - [30] F. Francica, S. Maniscalco, J. Piilo, F. Plastina, and K.-A. Suominen, Off-resonant entanglement generation in a lossy cavity, *Physical Review A* **79**, 032310 (2009).
 - [31] Y. Lin, J. P. Gaebler, F. Reiter, T. R. Tan, R. Bowler, A. S. Sørensen, D. Leibfried, and D. J. Wineland, Dissipative production of a maximally entangled steady state of two quantum bits, *Nature* **504**, 415 (2013).
 - [32] S. Shankar, M. Hatridge, Z. Leghtas, K. M. Sliwa, A. Narla, U. Vool, S. M. Girvin, L. Frunzio, M. Mirrahimi, and M. H. Devoret, Autonomously stabilized entanglement between two superconducting quantum bits, *Nature* **504**, 419 (2013).
 - [33] F. Benatti and R. Floreanini, Entangling oscillators through environment noise, *Journal of Physics A: Mathematical and General* **39**, 2689 (2006).
 - [34] C. H. Bennett, G. Brassard, S. Popescu, B. Schumacher, J. A. Smolin, and W. K. Wootters, Purification of noisy entanglement and faithful teleportation via noisy channels, *Phys. Rev. Lett.* **76**, 722 (1996).
 - [35] W. K. Wootters, Entanglement of Formation of an Arbitrary State of Two Qubits, *Physical Review Letters* **80**, 2245 (1998).
 - [36] S. A. Hill and W. K. Wootters, Entanglement of a Pair of Quantum Bits, *Physical Review Letters* **78**, 5022 (1997).
 - [37] G. Vidal and R. F. Werner, Computable measure of entanglement, *Physical Review A* **65**, 032314 (2002).
 - [38] M. B. Plenio, Logarithmic Negativity: A Full Entanglement Monotone That is not Convex, *Physical Review Letters* **95**, 090503 (2005).
 - [39] R. H. Dicke, Coherence in spontaneous radiation processes, *Phys. Rev.* **93**, 99 (1954).
 - [40] M. Gross and S. Haroche, Superradiance: An essay on the theory of collective spontaneous emission, *Physics Reports* **93**, 301 (1982).
 - [41] A. Auyuanet and L. Davidovich, Quantum correlations as precursors of entanglement, *Physical Review A* **82**, 032112 (2010).
 - [42] V. Gorini, A. Kossakowski, and E. C. G. Sudarshan, Completely positive dynamical semigroups of N-level systems, *Journal of Mathematical Physics* **17**, 821 (2008).
 - [43] G. Lindblad, On the generators of quantum dynamical semigroups, *Communications in Mathematical Physics* **48**, 119 (1976).
 - [44] H. J. Carmichael, *Statistical methods in quantum optics 1: master equations and Fokker-Planck equations* (Springer Science & Business Media, 2013).
 - [45] T. Astner, S. Nevlacsil, N. Peterschofsky, A. Angerer, S. Rotter, S. Putz, J. Schmiedmayer, and J. Majer, Coherent Coupling of Remote Spin Ensembles via a Cavity Bus, *Physical Review Letters* **118**, 140502 (2017).
 - [46] M. H. Fauzi, W. J. Munro, K. Nemoto, and Y. Hirayama, Double nuclear spin relaxation in hybrid quantum Hall systems, *Physical Review B* **104**, L121402 (2021).
 - [47] A. Angerer, K. Streltsov, T. Astner, S. Putz, H. Sumiya, S. Onoda, J. Isoya, W. J. Munro, K. Nemoto, J. Schmiedmayer, and J. Majer, Superradiant emission from colour centres in diamond, *Nature Physics* **14**, 1168 (2018).
 - [48] F. Anzà, B. Militello, and A. Messina, Tripartite thermal correlations in an inhomogeneous spin-star system, *Journal of Physics B: Atomic, Molecular and Optical Physics* **43**, 205501 (2010).
 - [49] A. Hutton and S. Bose, Mediated entanglement and correlations in a star network of interacting spins, *Physical Review A* **69**, 042312 (2004).
 - [50] C. Sabín and G. García-Alcaine, A classification of entanglement in three-qubit systems, *The European Physical Journal D* **48**, 435 (2008).
 - [51] K. Życzkowski, P. Horodecki, A. Sanpera, and M. Lewenstein, Volume of the set of separable states, *Phys. Rev. A* **58**, 883 (1998).